

Efficiency of rotating phase masks in the resolution

Andra Naresh Kumar Reddy^a, Mahdiah Hashemi^b

^a Samara National Research University, 443086, Moskovskoye Shosse, 34, Russia, Samara

^b College of Science, Fasa University, Fasa 74617-81189, Iran

Abstract

The redistribution of light energy in the receiving plane of the diffraction pattern by means of concurrent suppression of side-lobes and the amplification of the central disc by applying rotating phase masks at the exit pupil has been investigated. The magnitude of the suppression of side-lobes depends on the degree of the phase mask at the edge zones of the pupil. The mask is applied to achieve the side-lobe suppression on one side of the PSF. By applying a rotated mask, side-lobe suppression will occur on the other side of the PSF. The resolution of the object or signal under the optimum masking conditions is analysed by employing the standard characteristic parameters of the diffraction.

Keywords: diffraction; resolution; pupil function; point spread function; rotating phase-only pupil; airy pattern; FWHM; HWHM

1. Introduction

In recent years a lot of attention is drawn on the phase-only pupil functions, which are very effective in improving the resolution of an optical system compared to that of amplitude-only pupil functions. Rotational type phase-only masking is the deliberate modification of the amplitude transmittance of light in the focal plane of the optical imaging systems, with controlling the edge ringing effect. This mask changes the performance of the pupil plane by modifying its transmittance. Thus, it could affect the side-lobes by altering the aperture functions into suitable type, which can be technically possible in certain ways like shaping the pupil and shading the pupil. In earlier studies [1-4] the suppression of side-lobes are obtained at the cost of widening of the main peak. Recently, a significant number of research works are done [5-21] on the various mask designs, aims for high contrast imaging. Narrowing the main peak is very important for improving the resolving power of the instrument. In this paper, we follow this idea with applying rotating phase mask apertures which focus on the simultaneous suppression of optical side-lobes and sharpening the central peak in the required part of the diffraction pattern. Rotating the applied mask, enables us to control the resolution and side-lobe level in a counterpart of the diffracted field which is possible by integrating the proposed masks in imaging experiments. By employing rotating phase masks, the obtained point spread function (PSF) of the diffracted image is consisted of two parts: a part of the pattern with suppressed side-lobes and narrowed central peak and its counterpart with enhanced side-lobes and broad central peak. The PSF characteristics can be reversed by rotating the applied mask in a way to convert the blurred side of the pattern into the clear mode and vice versa. This kind of filter is very useful in resolving closely accompanied double lines and double stars. In other words, this kind of mask facilitates to detect the low intensity signal or image around the high intensity signal, which is one of the important solutions given for a common classical problem in wave optics or signal communication, known as two-point resolution. The present study paves a new way in the high resolution image formation, especially in telescopic observation applications and efficient electromagnetic wave communication. In this paper, we obtained PSF of the rotating phase masks analytically and show that by rotating the applied phase mask, the generated PSF will change its working area. The structure of the mask is divided into three zones: two edge phase masks of specified widths, with anti-phase functions relative to each other surrounding the transparent central zone with the uniform amplitude transmittance. Here we computed the efficiency of the mask in terms of well-known standard parameters like intensity of side-lobes, position and intensity of the main peak and the FWHM under various considerations.

2. Design and Formulation

According to the scalar wave diffraction theory, the intensity distribution of light radiation in the focal plane of an optical system is the Fourier transform of the phase mask pupil which light passes through it. In this paper, one- (1D) and two-dimensional (2D) phase masks and their relative rotated masks are introduced in Eq. 1 and Eq. 2, respectively. Schematic of these 1 and 2D applied masks are illustrated in Fig. 1.

$$1\text{D-Mask} = \begin{cases} \text{Left edge zone, } -i = e^{-i\pi/2}, & -\frac{1}{2} \leq r < -\frac{1}{2} + d \\ \text{Central zone} & -\frac{1}{2} + d \leq r \leq \frac{1}{2} - d \\ \text{Right edge zone, } +i = e^{i\pi/2}, & \frac{1}{2} - d < r \leq \frac{1}{2} \end{cases} \quad (1)$$

$$2D\text{-Mask} = \begin{cases} \text{Left edge zone, } -i = e^{-i\pi/2}, & r \rightarrow 1-d \text{ to } 1, -\frac{\pi}{2} \leq \varphi \leq \frac{\pi}{2} \\ \text{Central zone} & r \rightarrow 0 \text{ to } 1-d, 0 \leq \varphi \leq 2\pi \\ \text{Right edge zone, } +i = e^{i\pi/2}, & r \rightarrow 1-d \text{ to } 1, \frac{\pi}{2} \leq \varphi \leq \frac{3\pi}{2} \end{cases} \quad (2)$$

In which, ‘r’ is the coordinate of the pupil mask plane, ‘d’ is the width of the narrow edge strips in the 1D and the width of the semi-circular edge rings of the 2D mask filters (grey colour shaded regions in the Fig.1).

In case of applying the 1D phase mask, the diffracted field amplitude can be written as Eq. 3 [12]:

$$Y(z) = \int_{-\frac{1}{2}}^{-\frac{1}{2}+d} -i \exp(i 2zr) dr + \int_{\frac{1}{2}-d}^{\frac{1}{2}} T(r) \exp(i 2zr) dr + \int_{\frac{1}{2}}^{\frac{1}{2}+d} +i \exp(i 2zr) dr \quad (3)$$

The diffracted field amplitude which is contributed by the circular 2D rotating phase mask of Eq. 2, can be written as Eq. 4:

$$Y(z, \phi) = -i \int_{1-d}^1 \int_{-\frac{\pi}{2}}^{\frac{\pi}{2}} \exp(izr \cos(\phi - \varphi)) r dr d\varphi + \int_0^{1-d} \int_0^{2\pi} T(r) \exp(izr \cos(\phi - \varphi)) r dr d\varphi + i \int_{1-d}^1 \int_{\frac{\pi}{2}}^{\frac{3\pi}{2}} \exp(izr \cos(\phi - \varphi)) r dr d\varphi \quad (4)$$

Where, $z = k \sin\theta = (2\pi/\lambda) \sin\theta$ in which λ is the wavelength of the incident light, z is the dimensionless diffraction coordinate in the focal plane of the optical system which is connected to the angle of orientation θ and also specified y azimuth angle (ϕ). $T(r)$ is the amplitude transmittance of the central zone of the pupil mask function. It tends to maximum or unity for one-dimensional and two-dimensional rotating phase masks, which implies uniform transmittance over the central region of the phase mask pupil. Here we consider complex conjugated edge zones with uniform amplitude and opposite phase transmittances of $-i$ and $+i$. The resulting light intensity distribution in the receiving plane of the optical system is equal to the square modulus of $Y(z)$, $Y(z, \phi)$ corresponding to the slit and circular rotating phase apertures, respectively. When filtering takes place in the left side, the integral of the intensity square gives the minimum in the region $-\pi/3 < \phi < \pi/3$ and $\pi < k\sin\theta < 5\pi$. As the pupil function is rotated with an angle of 180 degrees, the phase functions at the edges of the pupil function can become reversed. This effect can modify the intensity of light distribution in the diffraction field of the optical system and the whole light pattern following the asymmetric mode nature. The parameter ‘d’ is also known as the control parameter of side-lobe suppression of the rotating asymmetric phase masks. The intensity of the PSF of the optical system, which is the real, measurable quantity, is given by Eq. 5 and 6 for the case of 1D and 2D masks, respectively:

$$I(z) = |Y(z)|^2 \quad (5)$$

$$I(z, \phi) = |Y(z, \phi)|^2 \quad (6)$$

The present study deals with the axial resolution of the PSF, which is done by employing the rotating phase masks. This study is technically very useful to increase the axial resolution in every direction around the PSF of the object of signal. The investigations of the results have been carried out by means of Eq. (5) and Eq. (6), which gives the image intensity distribution in the image plane of the optical system.

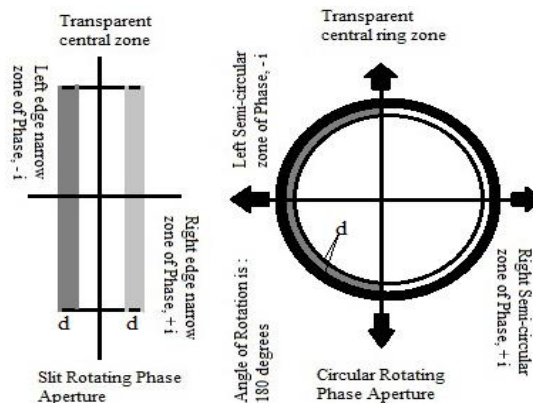


Fig.1. General Scheme of Rotating Phase masks: One-dimensional and Two-dimensional case.

3. Results

3.1. One-dimensional Rotating pupil mask

The results of investigations on the PSF of the optical system have been reported analytically in terms of the diffracted field characteristic parameters known as the central peak positions and its intensities, first side-lobe intensity on both sides of the PSF in addition to the resolution assessment parameters, full width at half maximum (FWHM) and half width at half maximum (HWHM). Here we employed the Gauss twelve-point quadrature method to obtain the point spread function distribution with the rotating phase masks. We developed and applied an iterative method of numerical integration to compute the peak positions and intensities. Fig.2 shows the modification of the PSF of the incident airy beam by applying the 1D phase mask of Fig. 1 in the front pupil. It is illustrated that for the $d = 0.06$, the side-lobes on the right hand side of the PSF are suppressed at the cost of enhancing the side-lobes in its counterpart. The Airy case is presented in dotted black line for the comparative study with the apodised cases. It is found that for the slit phase mask with 180° degrees of rotation, in the left hand side of the PSF the side-lobes will reach the zero level with a sharpened central peak while worsening the side-lobe level in the right hand side. The PSF curves in the Fig.2 demonstrate that as d sets to 0.06, the central peak is shifted towards the left side of the pattern compared to the incident airy beam distribution. Similarly the PSF curves in the Fig.3 explain that the central peak is shifted towards the right side of the pattern for rotated slit phase mask. It has shown in detail in the Fig.2 & Fig.3.

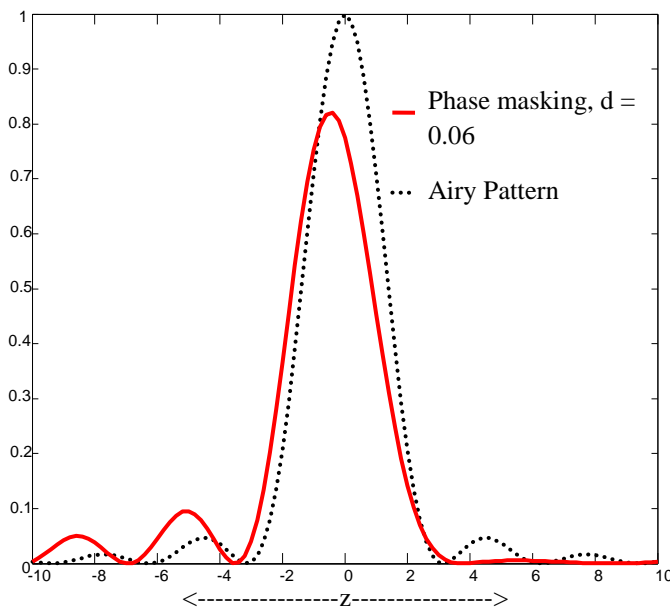


Fig.2. Intensity Profile of the PSF for the slit phase masks.

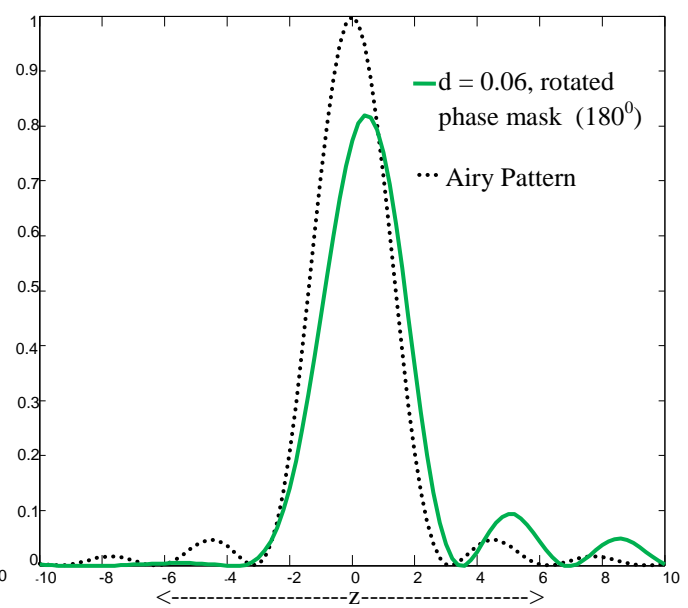


Fig.3. Intensity Profile of the PSF for the rotated slit phase masks.

Fig.2 illustrates the PSF for the one-dimensional phase mask, the incoherent Rayleigh limit or first minima position in the Airy pattern occurs at 3.1416. As d increases from 0 to 0.06 the first minima position on the right hand side is shifted from 3.1416 to 3.7711 whereas the first minima position on the left hand side of the main peak is shifted to -3.4999. The peak value position of the main lobe is shifted from 0 to -0.4584. The intensity of the first side-lobes on the right and the left sides of the main peak is calculated as 0.0056 and 0.0955. In the Fig.3 for the rotated slit with optimal anti-phase masking, the first minima positions on the left and right side of the pattern are found at -3.7711, 3.4999 respectively. So there exists a reversal effect in the pattern, has shown in the Fig.3 relatively with the pattern in the Fig.2. For the rotated slit phase mask of 0.06, the FWHM of the main peak is computed as 3.0160 and the HWHM on the good side (left) of the pattern is 1.1170. The HWHM on the bad side (right) of the pattern is measured as 1.8989. It is observed that for the rotated slit phase mask, the HWHM value on the good side is obtained smaller than the Airy case value (1.3915). The study concludes that the axial shape of the PSF of the optical system is modified with rotating anti-phase masks. In the case of an image of an object having one side with high contrast where it is required to keep the sharp edge of this side, and the counter side which is of no interest, a rotating phase mask can be used on the side of the image needing a high contrast.

3.2. Two-dimensional rotating pupil mask

Fig.4 illustrates that for the $d = 0.04$, the side-lobes on the right hand side of the pattern are found with the zero level intensity at the cost of the worsening its counterpart, relative to the incident the Airy pattern. It is observed that the phase mask with π degrees of rotation can switch the PSF into the other mode, where the left hand side of the pattern is found with the suppressed side-lobes and the sharpened central peak at the cost of enhanced side-lobes and broadened central peak on the right hand side of the pattern which leads to central peak frequency shift. The PSF in the blue curve explains that as for ' d ' equals to 0.04, the PSF pattern is shifted towards the right hand side, whereas the PSF in the red curve is shifted towards the left hand side of the pattern for the rotated circular phase mask. It can be seen in more details in the Fig.4.

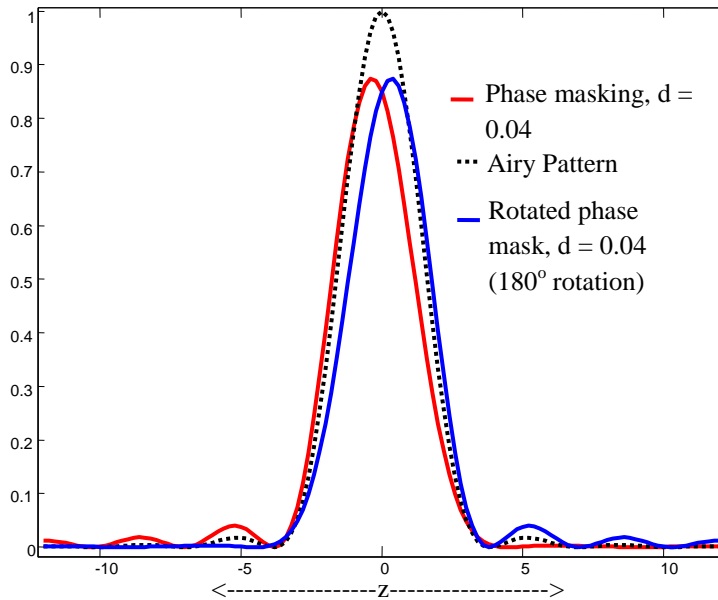


Fig.4. Intensity Profile of the PSF curves for optimized two-dimensional rotating phase masks.

In the Airy case ($d = 0$) the first minima position takes place in 3.8317 (incoherent Rayleigh limit). As d increases from 0 to 0.04 (optimum anti-phase masking) the first minima position (PSF curve in red) on the right and left side of the pattern is found at 4.4375, -3.8192, respectively, and the peak position of the main lobe is shifted from 0 to -0.3461. In the presence of the phase mask the intensity of enhanced first side-lobe (on the left side) is measured as 0.0027 where as by applying the rotated phase masks the first side-lobe intensity on the right side is measured as 0.0399. In the Airy case the intensity of the first side-lobe is measured as 0.0174. However, similar results are noticed when the phase mask is rotated with an angle of π but the peak positions, peak values and the first side-lobe intensity values on the left hand side of the pattern are replaced by the corresponding values on the right hand side of the pattern and vice versa. In this case, the left hand side of the pattern (blue PSF curve) is found with the flattened side-lobes and narrowed main peak is obtained at the cost of enhanced side-lobes and broadened main peak on the right hand side. It emphasizes that how effective is rotating phase masks in suppressing the side-lobes on the other side of the main peak. This facilitates to detect the presence of extremely faint companion in every direction around the bright companion in the spectrum. The FWHM value of the Airy PSF is 3.2327. In the case of the optimum rotated phase masking pupil, the FWHM value of the PSF is measured as 3.2781, in addition to this we introduced and computed the HWHM as the new criterion to assess the axial resolution of the PSF. It is the width of the main peak from diffraction centre where the peak intensity becomes 50% of its maximum value. For the rotated phase mask, the HWHM (for the profile curve in blue) on the left and the right sides of the PSF are measured as 1.3568, 1.9213 correspondingly. It concludes that the decreased HWHM on the left hand side is obtained at the cost of increased HWHM on the counter side and vice versa for the red PSF curve. The HWHM value on the left side of the PSF is obtained less than that of Airy case (1.6163).

3.3 Two-point resolution study: Two-dimensional pupil mask

Fig. 5 illustrates the intensity distribution as a function of 'z' for different values of point separation Z_0 . Considering the Sparrow criterion, the resolution is booked when the second derivative of the composite image intensity distribution of the optical system vanishes at a certain point between two Gaussian image points, that point should be a solution for the first derivative of the total image intensity distribution becoming zero. In the modified Sparrow criterion sense the smallest point separation where the object points are resolving is equal to Z_0 . In this study the degree of coherence is equal to zero (the incoherent illumination) and the intensity ratio of two object points is assumed to keep 0.6. Fig.5 shows various intensity curves for $Z_0 = 4$ which is chosen in a way that it is greater than the incoherent Rayleigh limit ($3.83 = 1.22\lambda/D_{\text{mask diameter}}$), the incoherent Sparrow limit (2.97) and less than the coherent Sparrow limit (4.60) [21]. For the phase mask with $d = 0.04$, as the point separation Z_0 sets from 4.0 to 4.5, the intensity of the central dip increases to the higher value. The magnitude of this effect is improved by employing the rotated phase mask. In other words for the same value of d , as the pupil function is modified into the rotated phase mask, then the Sparrow limit decreases. It conveys that the resolution is increased. Similar trend result is noticed for the point separation $Z_0 = 4.5$. It is concluded that by employing the rotating asymmetric phase mask the maxima of the high intensity PSF and the low intensity PSF are almost correctly correspond to the real Gaussian image points. It is also observed that initially the position of the dip shifts toward the left hand side of the pattern is found with enhanced side-lobes are obtained at the cost of the suppressed side-lobes on the right hand side of the pattern, whereas by rotating the asymmetric phase mask the position of the dip on the intensity curves shifts toward the right hand side of the profile, is known as bad side is obtained at the cost of the counter side (left side). The side-lobes found on the left hand side which are much flatter than the unapodized ones. This study is very useful in astronomical observations to detect the low intensity object in any direction around the bright intensity object.

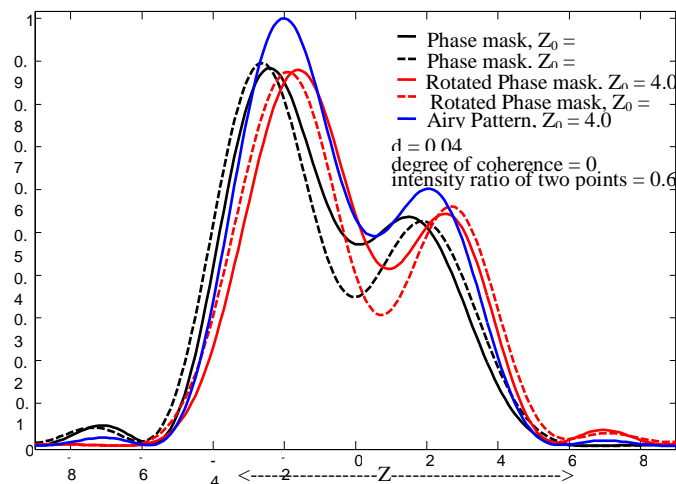


Fig.5. Intensity distribution of two unequal bright points under the incoherent light illumination.

4. Conclusion

It concludes that by employing the rotating phase masks it is possible to obtain the object having sharp resolution on one side means an abrupt change of the side into the good side in which the side-lobes are eliminated. This effect continues as long as it is required in the experiment or system. It is also observed that for optimal rotating anti-phase mask the side-lobes are obtained with 98% of intensity suppression, tailored the axial shape of the PSF. It is emphasized that in the presence phase mask, the lower HWHM values are obtained relatively with the Airy case. By rotating the phase masks of slit or circular type, we can detect the direct image of the low intensity object in all directions around the high intensity object in the sense of acquiring the PSF of suppressed side-lobes side on alternatively the right and left of high intensity object facilitates obtaining the high contrast image of the object or signal under closer examination of the imaging or detector instrument. Our applied design is highly useful to achieve the axial superresolution in confocal microscopy. If we modify the limits of the phase mask with the help of additional parameters we can improve the results in terms of the application context. Further studies on experimental fabrication of the rotating asymmetric phase mask are being conducted out.

References

- [1] Jacquinot, P. Roizen-dossier, B. Apodization. Progress in Optics, 1964. - Vol.3. - P. 29-32.
- [2] Mills, JP. Thompson, BJ. Selected papers on apodization: coherent optical systems - Washington: "SPIE Optical Engineering Press" Publisher, 1996. - Vol.119.
- [3] Barakat, R. Application of apodization to increase Two-point resolution by Sparrow criterion under incoherent illumination. J. Opt. Soc. Am., 1962. - Vol.52. - P. 276-283.
- [4] Barakat, R. Solution to the Lunenberg Apodization problems. J. Opt. Soc. Am., 1962. - Vol.52. - P. 264-272.
- [5] Cheng, L. Siu,GG. Asymmetric apodization. Measurement and Technology, 1991. - Vol.2(3). - P. 198-202.
- [6] Siu, GG. Cheng, L. Chiu, DS. Improved side-lobe suppression in asymmetric apodization. J. Phys. D: Applied Physics, 1994. - Vol.27(3). - P. 459-463.
- [7] Siu, GG. Cheng, M. Cheng, L. Asymmetric apodization applied to linear arrays. J. Phys. D: Applied Physics, 1997. - Vol. 30 (5). - P. 787-792.
- [8] Zervas, MN. Tarvener, D. Asymmetrically apodised linear chirped fiber gratings for efficient pulse compression. Fiber and Integrated Optics, 2000. - Vol.19 (4). - P. 355-365.
- [9] Khonina, SN. Kazanskiy, NL. Volotovskiy, SG. Vortex phase transmission function as a factor to reduce the focal spot of high-aperture focusing system. Journal of Modern Optics, 2011. - Vol.58(9). - P. 748-760.
- [10] Khonina, SN. Kazanskiy, NL. and Volotovskiy, SG. Influence of vortex transmission phase function on intensity distribution in the focal area of high-aperture focusing system. Optical Memory and Neural Networks (Information Optics), 2011. - Vol.20(1). - P. 23-42.
- [11] Khonina, SN. Nesterenko, DV. Morozov, AA. Skidanov, RV. Soifer, VA. Narrowing of a light spot at diffraction of linearly-polarized beam on binary asymmetric axicons. Optical Memory and Neural Networks (Information Optics), 2012. - Vol.21(1). - P. 17-26.
- [12] Keshavulu Goud, M. Komala, R. Naresh Kumar Reddy, A. and Goud, SL. Point spread function of asymmetrically apodised optical systems with complex Pupil filters. Acta Physica Polonica A, 2012. - Vol.122(1). - P. 90-95.
- [13] Naresh Kumar Reddy, A. Karuna Sagar, D. Point spread function of optical systems apodised by a semicircular array of 2D Aperture functions with asymmetric apodization. Journal of Information and Communication Convergence Engineering, 2012. - Vol.12(2). - P. 83-88.
- [14] Kowalczyk, M. Zapata-Rodriguez, CJ. Martinez-Corral, M. Asymmetric apodization in confocal scanning systems. Applied Optics, 1998. - Vol.37(35). - P. 8206-8214.
- [15] Yang, W. Kotinski, AB. One-sided achromatic phase apodization for imaging of extra solar planets. The Astrophysical Journal, 2004. - Vol.605(2). - P. 892-901.
- [16] Khonina, SN. Pelevina, EA. Reduction of the focal spot size in high-aperture focusing systems at inserting of aberrations. Optical Memory and Neural Networks (Information Optics), 2011. - Vol.20(3). - P. 155-167.
- [17] Khonina, SN. Ustinov, AV. and Pelevina, EA. Analysis of wave aberration influence on reducing the focal spot size in high-aperture focusing system. J. Opt., 2011. - Vol.13. - P. 13p.
- [18] Khonina, SN. and Ustinov, AV. Sharper focal spot for a radially polarized beam using ring aperture with phase jump. Journal of Engineering, 2013. - 8p.
- [19] Falconi, O. The limits to which double lines, Double stars, and Disks can be resolved and measured. J. Opt. Soc. Am., 1967. - Vol.57(8). - P. 987.
- [20] Andrew Watson, B. Computing human optical Point spread functions. Journal of Vision, 2015. - Vol.15(2). - P.1-25.
- [21] Asakura, T. Resolution of two unequally bright points with partially coherent light. Nouv. Rev. Opt, 1974. - Vol.5. - P. 169-177.